Cancer Science
The official journal of the Japanese Cancer Association

In vivo bioimaging tracks conditionally replicative adenoviral replication and provides an early indication of viral antitumor efficacy

Julia Davydova,[1,4] Tatyana Gavrikova,[2] Eric J. Brown,[1] Xianghua Luo,[3] David T. Curiel,[2] Selwyn M. Vickers[1] and Masato Yamamoto[1]

[1]Division of Basic and Translational Research, Department of Surgery, University of Minnesota, Minneapolis, Minnesota; [2]Division of Human Gene Therapy, University of Alabama at Birmingham, Birmingham, Alabama; [3]Division of Biostatistics, School of Public Health, University of Minnesota, Minneapolis, Minnesota, USA

(Received September 2, 2009/Revised October 8, 2009/Accepted October 12, 2009/Online publication November 8, 2009)

***In vivo* monitoring of conditionally replicative adenovirus (CRAd) replication and assessing its correlation to CRAd biological effects are necessary for the clinical development of gene therapy. Non-invasive bioimaging is one current approach which can monitor *in vivo* CRAd replication and functional effect. Here we describe a novel cyclooxygenase-2 (Cox2) promoter-controlled CRAd that was modified to contain firefly luciferase in its E3 region; this modification permitted serial bioluminescence imaging of viral replication *in vitro* and *in vivo*. *In vitro* luciferase expression correlated with viral replication and cytolytic effect. *In vivo* bioluminescence imaging showed dynamic representation of the viral replication level in athymic nude mice bearing subcutaneous tumor xenografts. Importantly, *in vivo* luciferase bioluminescence measured 6 days after viral administration significantly correlated with CRAd antitumor effect at day 36. Thus, our system could detect viral replication and predict *in vivo* therapeutic outcome based on early imaging. Further development of this approach may improve patient safety, enhance clinical trial conduct, and provide mechanistic insight into CRAd function *in vivo*. (*Cancer Sci* 2010; 101: 474–481)**

Conditionally replicative adenoviruses (CRAds) are promising anticancer agents designed to exploit tumor-selective replication followed by lysis of the tumor and lateral spread of viral progeny *via* infection of neighboring tumor cells.[1,2] As encouraging as the concept of virotherapy may appear, clinical trials have not yet validated the competence of oncolytic adenoviral vectors as a single-agent therapy against cancer.[3–5] Experience from clinical trials has indicated that little is known about the function and biodistribution of oncolytic adenoviruses *in vivo*.[6] Currently, invasive and cumbersome tissue biopsy is the standard approach for monitoring viral replication in patients.[7–9] A simple, noninvasive method to determine CRAd distribution and to accurately measure CRAd replication *in vivo* would overcome this limitation. Such a method would also detect cancer-specific *versus* ectopic CRAd replication, thereby improving the clinical safety of gene therapy and facilitating more rapid development of new oncolytic CRAds.

We previously reported that adenoviral major late promoter-driven (MLP) expression of fluorescent protein accurately represents AdΔE3ADPEGFP replication *in vitro* and *in vivo*.[10] In that vector structure, the enhanced green fluorescent protein (*EGFP*) reporter gene placed in the E3 region was controlled by MLP, and enhanced adenovirus (Ad) oncolysis was mediated by overexpression of the adenoviral death protein (ADP). Expression of a fluorescent signal from the adenovirus E3 region follows a late profile due to control by the major late promoter[10] and is therefore consistent with the replication cycle – a property that may be exploited to monitor adenovirus replication. Although the EGFP reporter was operative in our detection scheme for monitoring adenovirus replication, we were conscious of its major limitation for *in vivo* studies, namely poor detectability deep in tissue.

For this paper, we use firefly luciferase (Luc) to monitor viral replication. Firefly luciferase has several benefits over green fluorescent protein: it has a wider dynamic range, it does not require excitation light, its background is extremely low, and it can be detected deeper in tissue.[11–14] The ΔE3 vector structure was optimized for better monitoring and oncolytic features, and then recombined with a cyclooxygenase-2 (Cox2) promoter-driven E1 expression cassette. The lead vector was tested *in vitro* and *in vivo* for how well it represented viral replication and antitumor effect. In an *in vivo* therapeutic study employing Cox2-positive and Cox2-negative tumor subcutaneous xenograft nude mice models, we observed a strong correlation between early time-point imaging data and later antitumor effect.

In this work, we apply Luc-equipped CRAd as an imaging tool to monitor viral replication and oncolytic functionality, but also to predict final antitumor effect based on earlier time-point analysis. We showed that by combining adenovirus replication-mediated oncolysis, enhanced cytocidal effect, tumor selectivity, and imaging capability to track Ad replication and possibly predict therapeutic outcome, we present a new generation of CRAds which could be translated into clinical trials and greatly improve functionality and safety of gene therapy approaches in cancer medicine.

Materials and Methods

Cell lines. Human A549 lung carcinoma, A431 epidermoid carcinoma,[15] and mouse BNL-1NG-A.2 (BALB/c transformed hepatoma, hAd replication nonpermissive control) were obtained from the American Type Culture Collection (Manassas, VA, USA) and grown in DMEM (Mediatech, Manassas, VA, USA). BT474 breast cancer cells were grown in RPMI-1640 (Mediatech) supplemented with bovine insulin (0.01 mg/mL; Life Technologies, Rockville, MD, USA).

Adenoviral vectors. We incorporated the luciferase gene into the adenoviral E3 region because of the well-documented high level of transgene expression from this location.[10,16–19] Four test adenovirus type 5 vectors containing a Luc reporter in the E3 region were constructed using pShuttleΔE3ADPKanF2 cloning.[10] Briefly, ADP was maintained in the adenoviral E3 region while all other nonessential E3 genes such as 12.5 K, 6.7 K, gp19K, RID-α and RID-β, and 14.7 K were deleted. This

[4]To whom correspondence should be addressed.
E-mail: davyd003@umn.edu

doi: 10.1111/j.1349-7006.2009.01407.x

liberated ~2.3 kb of cloning capacity to accommodate the reporter. Luciferase from pGL3-Basic (Clontech, Palo Alto, CA, USA) was cloned in the forward direction of XbaI and SalI sites in the pShuttleΔE3ADPKanF2 vector. The shuttle vector was linearized with AatII and PacI, recombined with Ad5 DNA in BJ5183 bacteria, and SwaI cleaved to remove kanamycin resistance. The resultant plasmids were then either recombined with PmeI-linearized pShuttleCox2CRAd F[20,21] and transfected into 911 cells to generate Cox2-based CRAds with Luc imaging capability (*Cox2CRAdΔE3ADPLuc*), or they were linearized with PacI and transfected to generate non-selective vectors with ΔE3 luciferase reporters (*WtΔE3ADPLuc*). Information on detailed procedures taken to construct the *WtΔE3ADPLuc* counterpart lacking pA after the luciferase gene (*WtΔE3ADP-Luc_noPA*) and the wild-type replication vector with the luciferase-pA cassette in the E3 region but without ADP (*WtΔE3Luc_noADP*) is available upon request.

A wild-type adenovirus (*Ad5Wt*) was used to compare the oncolytic potency of these four ΔE3Luc vectors; a replication-incompetent Cox-2 promoter-driven luciferase expression vector (*AdCox2LLuc*) was used as a non-replicative control.[22]

All viruses were propagated in A549 cells, purified by double cesium chloride density gradient ultracentrifugation, and dialyzed in PBS with 10% glycerol. The viral particle/plaque forming unit ratios for these vectors were in the range of 12–20.

Analysis of replication-dependent luciferase expression and viral DNA quantitation. To analyze replication-mediated Luc expression, cells (4000 cells/well) cultivated in 96-well plates were infected with the indicated viruses at 0.1 viral particle (vp)/cell. After 3 h, the infection medium was replaced with 2.5% FBS medium. At days 2, 4, 7, and 9 after infection, culture supernatant was transferred into new 96-well plates and frozen until viral DNA quantitation analysis. Cell monolayers were washed with PBS, lysed, and Luc activity was measured using a Luciferase Assay System (Promega, Madison, WI, USA). Viral DNA was extracted from the supernatant (QIAamp DNA Blood Mini Kit; Qiagen, Valencia, CA, USA) and then quantitated by Taqman real-time PCR with E4 primers (LightCycler System; Roche Applied Science, Indianapolis, IN, USA) [20] All experiments were performed in triplicate.

***In vitro* analysis of adenoviral cytolysis.** At day 10 after infection, infected cells were fixed in 10% buffered formalin and stained with 1% crystal violet in 70% ethanol. Crystal violet stained cells were washed with water and dried.

Detection of Cox2 promoter-dependent CRAd replication. Cultured cells were infected with 0.1 vp/cell. At day 2 after infection, the cells were lysed, and luciferase activity was determined with the Luciferase Assay System (Promega). Experiments were performed in triplicate and standardized with protein concentration quantitated by the DC protein assay (Bio-Rad, Hercules, CA, USA).

***In vivo* detection of luciferase bioluminescence.** A549 or BNL-1NG-A.2 cells (2.0×10^6) were administered into the flanks of 6–8 week old female ncr/nu nude mice (Frederick Cancer Research, Frederick, MD, USA). When tumor nodules achieved a diameter of 6–10 mm, ΔE3Luc vectors were injected intratumorally (4×10^9vp in 50 μL PBS) or intravenously (5×10^9vp in 50 μL PBS). *In vivo* Luc expression then was assessed over a 5 week time-course. At each assessment, individual mice were injected intraperitoneally with 3 mg D-Luciferine (Molecular Imaging Products, Bend, OR, USA), placed under 2% isoflurane anesthesia, and positioned in the imaging chamber of a custom-built optical imaging system.[10] This system consists of a cryogenically cooled, back-illuminated Princeton Instruments VersArray:1KB digital CCD camera (Roper Scientific, Trenton, NJ, USA) with a liquid nitrogen autofill system mounted on top of a light-tight enclosure. The whole-body images were acquired repetitively during the 9- to 11-min intervals after D-luciferine injection at f/1.2 with 60 s exposure time (WinView/32 software; Roper Scientific). The images with peak relative light units (RLU) were taken for further analysis. A brightfield image was also taken at f/16 for 0.05 s at the lowest light level. The imaging data were displayed as a pseudocolored luminescence intensity image overlaid on a brightfield image of the entire mouse body. Index color image overlays were performed in Photoshop 7.0 (Adobe, Seattle, WA, USA).

***In vivo* antitumor effect in a mouse xenograft model.** A549 and A431 cells (2.0×10^6) were inoculated into the flanks of female ncr/nu nude mice (6–8 weeks of age; Frederick Cancer Research). When the tumor nodules achieved a diameter of 8–10 mm, a single-virus dose was injected intratumorally (10^{10}vp in 50 μL PBS). Tumor diameter and bioluminescent light imaging were measured bi-weekly. Tumor volume was calculated using [tumor volume = (width^2 × length)/2]. Bioluminescent light imaging was facilitated by the custom-built optical imaging system as described above.

Statistical methods. Statistical analysis of CRAd efficacy *in vitro* and *in vivo* was performed with a two-tailed *t*-test. Data are expressed as a mean ± SD of at least three samples. Analysis of the correlation between bioluminescence values and tumor volumes was done with the nonparametric Spearman's rank correlation. The linear regression was performed on the natural-log transformed variables of luciferase peaks at day 6 and tumor volumes at day 36 with the latter being the dependent variable and the former being the independent variable. Results were considered statistically significant when $P < 0.05$.

Results

***In vitro* monitoring of CRAd replication and luciferase expression.** Four oncolytic adenoviral vectors containing the luciferase reporter gene were successfully constructed: (i) a wild-type vector with an E3 region containing ADP and the Luc-polyadenylation signal (pA) cassette (WtΔE3ADPLuc); (ii) a WtΔE3ADPLuc counterpart lacking a pA after the *Luc* gene (WtΔE3ADPLuc_nopA); (iii) a wild-type vector with an E3 region containing the Luc-pA cassette but not the ADP (WtΔE3Luc_noADP); and (iv) a Cox2 promoter-controlled vector with an E3 region containing both ADP and Luc-pA (Cox2CRAdΔE3ADPLuc) (Fig. 1).

To prove the replication-dependent expression of the luciferase reporter placed in the E3 region, we used human adenovirus replication-permissive and non-permissive cell lines (human lung adenocarcinoma A549 cells and mouse hepatoma BNL-1NG-A.2 cells, respectively). Cultured A549 and BNL-ING-A.2 cells were infected with 0.1 vp/cell to avoid immediate cytotoxicity, and cell luciferase activity was measured 1 to 9 days later. These four CRAds increased Luc activity in A549 cells in a time-dependent manner; no Luc expression occurred in non-permissive BNL-1NG-A.2 cells. Lower Luc expression was measured in A549 cells infected with WtΔE3Luc_noADP while WtΔE3ADPLuc, WtΔE3ADPLuc_nopA, and Cox2CRAD ΔE3ADPLuc showed similar high levels of bioluminescence (Fig. 2a).

Adenoviral E4 DNA copy number was measured in cell culture media to correlate luciferase expression with CRAd replication. The time-dependent increases in luciferase signal correlated well with viral DNA copy number in replication-permissive A549 cell, as both log phases occurred at the same time. As expected, non-permissive BNL-1NG-A.2 cells showed no viral replication (Fig. 2b).

Crystal violet assay for killing ability determination. To analyze the oncolytic effect of the four test vectors, A549 and BNL-1NG-A.2 cells were exposed to 0.1 and 1.0 vp/cell; these low titers being chosen to allow multiple cycles of viral replication. Ten days after exposure, crystal-violet staining showed

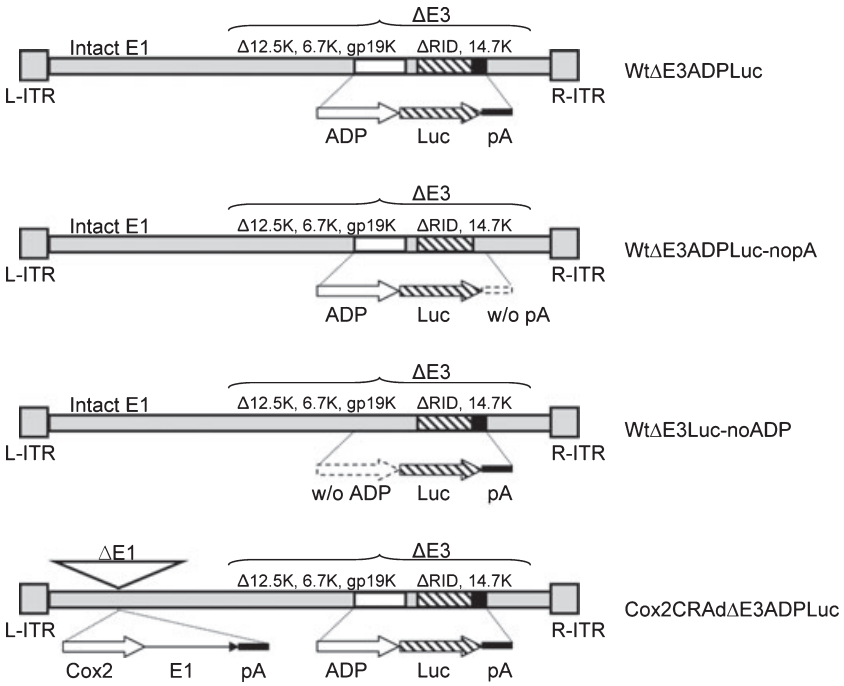

Fig. 1. Structure of oncolytic adenoviral vectors with a major late promoter-driven luciferase expressing cassette. ADP, adenoviral death protein; Cox2, cyclooxygenase-2; CRAd, conditionally replicative adenovirus; Luc, firefly luciferase; pA, polyadenylation signal.

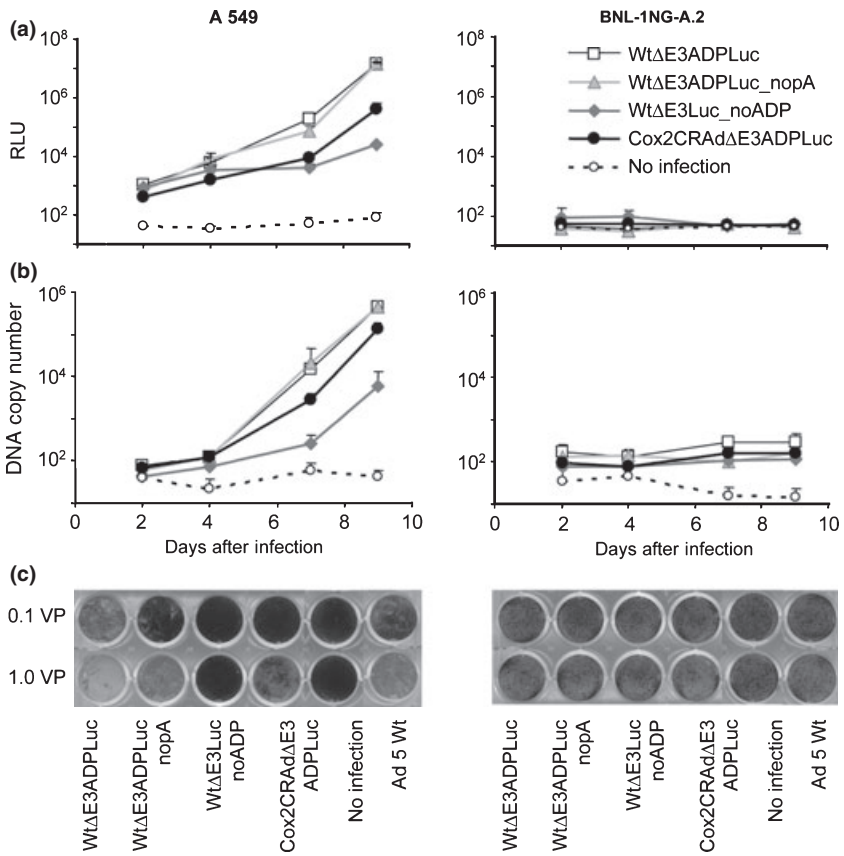

Fig. 2. Correlation of luciferase (Luc) expression, adenoviral replication, and oncolytic effect *in vitro*. (a) A549 cell line (human adenovirus [hAd] replication-permissive) and BNL-1NG-A.2 cells (replication non-permissive control) were infected with ΔE3Luc adenoviruses at 0.1 viral particle (vp)/cell. Luminescence was detected on days 2, 4, 7, and 9. In A549 cells, adenoviruses showed transgene expression augmentation in a time-dependent manner. The vector structure lacking adenoviral death protein (ADP) resulted in decreased reporter expression. No differences in luciferase expression were noticed after infection with pA (+) and pA (–) vectors. No luciferase expression was observed in BNL-1NG-A.2 replication non-permissive cells. Cox2, cyclooxygenase-2; CRAd, conditionally replicative adenovirus; RLU, relative light units. (b) The detected luciferase signal closely correlates with the viral DNA quantity resulting from viral replication. (c) Oncolytic potency of ΔE3Luc vectors in cancer cells. A549 and BNL-1NG-A.2 cells were infected with ΔE3Luc adenoviruses and Ad5 wild-type vector as a control at 0.1 and 1.0 vp/cell. Ten days later, the cells were fixed and stained with crystal violet. All vectors with the exception of the structure without ADP demonstrated replication and subsequent oncolysis in A549 cells, but not in the hAd replication non-permissive BNL-1NG-A.2 cell line.

oncolytic death in A549 cells infected with WtΔE3ADPLuc, WtΔE3ADPLuc_nopA, and Cox2CRAdΔE3ADPLuc but not A549 cells exposed to WtΔE3Luc_noADP. This confirms the crucial role of ADP in cytophatic effect. Vector WtΔE3ADPLuc outperformed Cox2CRAdΔE3ADPLuc and wild-type Ad5, on the other hand, Cox2-controlled CRAd was as strong as Wt Ad5. No oncolysis was observed in hAd non-permissive BNL-1NG-A.2 cells (Fig. 2c).

***In vitro* analysis of Cox2-driven viral replication.** A549, a cell line expressing high levels of Cox2; BT474, a breast cancer cell expressing low levels of Cox2; and A431, a lung cancer cell expressing low levels of Cox2, were used to test the

doi: 10.1111/j.1349-7006.2009.01407.x

promoter status and the Cox2-dependent replication of Cox2CRAdΔE3ADPLuc. As expected, significantly lower levels of luciferase expression occurred in the two Cox2-negative cell lines exposed to Cox2CRAdΔE3ADPLuc when compared to A549 cells or to cells exposed to wild-type replication vector (Fig. 3).

Bioluminescent detection of *in vivo* CRAd replication and oncolysis. Whether CRAd vectors containing Luc reporters could track *in vivo* deep tissue viral replication and oncolysis was tested next. Since systemic adenovirus injections have less ability to reach subcutaneous tumors, as compared with local administration, we analyzed both routes of virus administration. Athymic nude mice were inoculated with either A549 or BNL-1NG-A.2 subcutaneous tumors. After tumors reached a diameter of 6–10mm, half of the mice bearing A549 tumors and BNL-1NG-A.2 tumors were injected intratumorally with Cox2CRAdΔE3ADPLuc; remaining mice were injected in the tail vein. During the following 5 weeks, the mice were injected intraperitoneally with D-Luciferine and luciferase activity was measured using noninvasive bioluminescence imaging.

Luciferase bioluminescence occurred as early as the day after intratumoral injection of vector into A549 nodules; bioluminescence peaked between days 5 and 13 in intratumorally treated mice, and persisted for up to 4 weeks (Fig. 4a). In contrast, tumor-associated bioluminescence started at day 5 when vectors were administered intravenously, peaked between days 13 and 20, but also persisted for 4 weeks (Fig. 4b). Two additional important points are worth mentioning. First, no luciferase bioluminescence was measured in mice bearing non-permissive BNL-1NG-A.2 xenografts that were challenged with the WtΔE3ADPLuc or the Cox2CRAdΔE3ADPLuc vectors (data not shown). Second, ascites developed in one mouse bearing an A549 subcutaneous tumor 13 days after intratumoral injection with Cox2CRAdΔE3ADPLuc and a pronounced bioluminescent signal was detected throughout its abdomen. Whole-body luciferase imaging was performed on this mouse for 20 days after

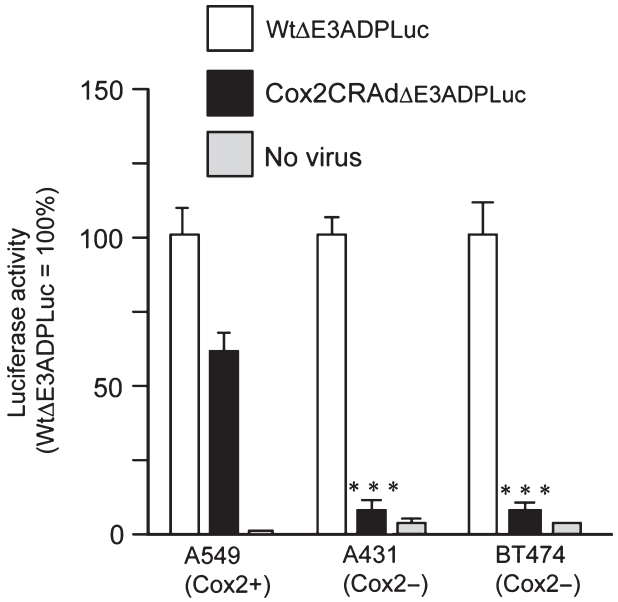

Fig. 3. Luciferase (Luc) reporter represents selective cyclooxygenase-2 (Cox2) promoter-dependent replication in cancer cell lines. Cox2-positive (A549) and Cox2-negative (A431 and BT474) cells were infected with WtΔE3ADPLuc and Cox2CRAdΔE3ADPLuc at 0.1 viral particle (vp)/cell. Luciferase activity was measured 2 days after infection. The high level of luciferase expression was observed in all cell lines after infection with WtΔE3ADPLuc. The infection with the Cox2-controlled E1 region vector resulted in efficient reporter expression only in the Cox2-positive A549 cell line while minimal luciferase activity was observed in Cox2-negative A431 and BT474. Data are shown as percentages of relative light units (RLU) per mg protein in relation to that of WtΔE3ADPLuc. Error bars represent SD calculated from three replicates; $*P < 0.05$, $**P < 0.005$, $***P < 0.001$. CRAd, conditionally replicative adenovirus.

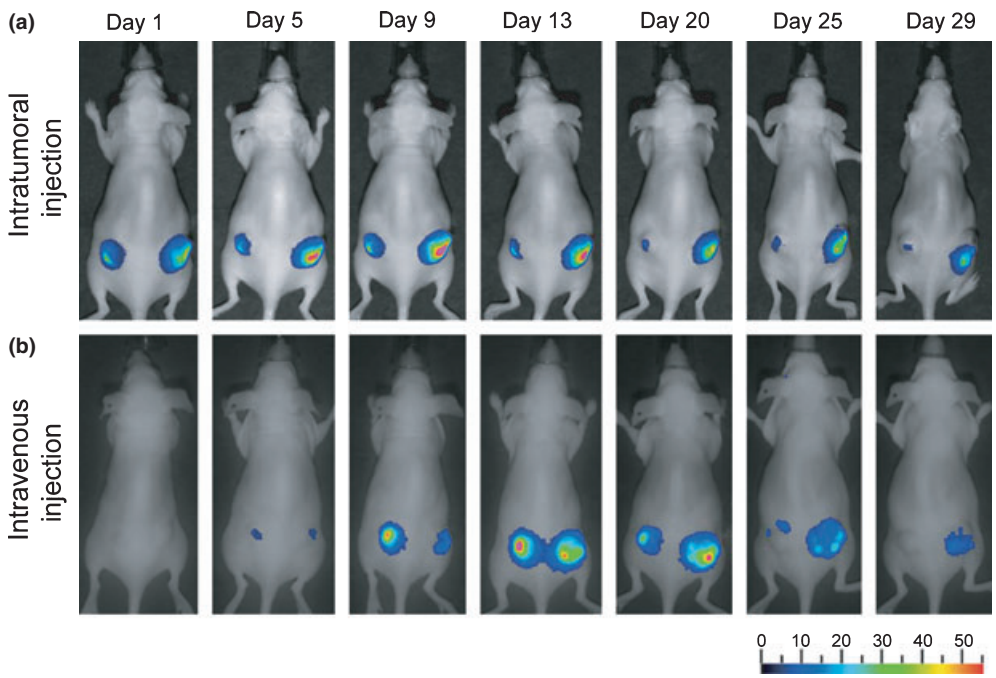

Fig. 4. Bioluminescent imaging tracks adenoviral replication and distribution after intratumoral (a) and intravenous (b) virus administration in A549 lung cancer xenografts. Nude mice were inoculated with A549 lung cancer cells and 3 weeks later injected with Cox2CRAdΔE3ADPLuc. The luciferase signal after intratumoral injections (4×10^9 viral particle (vp)/tumor) was observed starting from day 1, peaked around days 5 to 13, and resulted in persistence of alive imaging of bioluminescence over 4 weeks. Intravenous delivery (5×10^9 vp/mouse) produced the bioluminescent signal by day 5, which peaked between day 13 and 20, and persisted until day 29. ADP, adenoviral death protein; Cox2, cyclooxygenase-2; CRAd, conditionally replicative adenovirus; Luc, firefly luciferase.

Cox2CRAdΔE3ADPLuc treatment, at which time the mouse was sacrificed, its internal organs isolated, and imaged *ex vivo*. Post-mortem bioluminescence imaging identified metastases in the intestines, stomach, diaphragm, and peritoneum (Supporting Information Fig. S1).

***In vivo* imaging of Cox2CRAdΔE3ADPLuc replication can predict viral antitumor efficacy.** Finally, athymic mice bearing A549 (Cox2-positive) and A431 (Cox2-negative) flank tumors were used to test the *in vivo* tumoricidal efficacy of ΔE3Luc vectors. Tumor-bearing mice were injected intratumorally with 10^{10} vp of WtΔE3ADPLuc, Cox2CRAdΔE3ADPLuc, and the non-replicative control, AdCox2LLuc. Tumor size measurement and bioluminescent imaging were performed bi-weekly for the following 5 weeks. Tumor growth regression was observed in A549-bearing mice after treatment with ether Cox2 CRAdΔE3ADPLuc or WtΔE3ADPLuc vectors. However, significant tumor regression was registered only on day 18 after adenoviral injections, as compared with the group that received the non-replicative AdCox2LLuc vector. There was no significant difference in A549 tumor volumes between Cox2CRAdΔE3 ADPLuc- and WtΔE3ADPLuc-treated mice throughout the experiment. In contrast, in the Cox2-negative (A431) xenografts, Cox2CRAdΔE3ADPLuc resulted in insignificant tumor shrinkage compared to the control mice, while significant tumor regression occurred with the wild-type replication vector (Fig. 5). The bioluminescence signal in A549-bearing mice treated with either the Cox2-controlled vector or wild-type vector WtΔE3ADPLuc and in A431 mice treated with WtΔE3ADPLuc persisted until the last day (day 36) of the experiment, when all mice were sacrificed due to tumor volume in control groups.

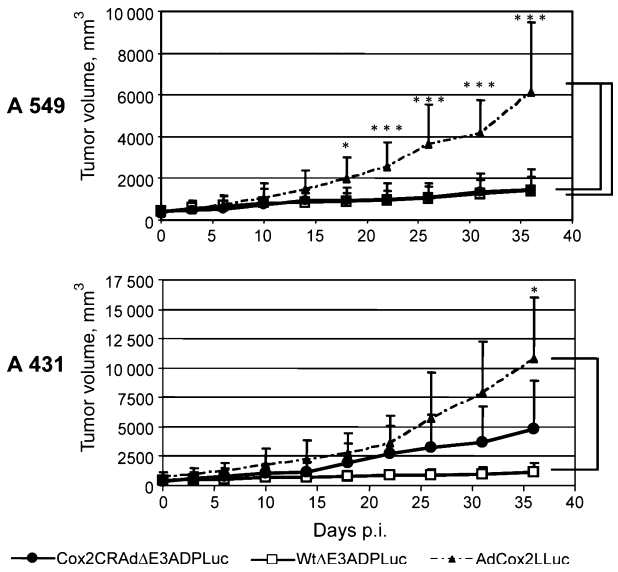

Fig. 5. Therapeutic effect of ΔE3Luc vectors in a mouse xenograft model. Cyclooxygenase-2 (Cox2)-positive A549 tumors and Cox2-negative A431 tumors were injected with 10^{10} viral particle (vp)/tumor of a single dose of WtΔE3ADPLuc, Cox2CRAdΔE3ADPLuc, or non-replicative AdCox2LLuc as a control vector. Significant tumor growth suppression was observed only on day 18 after adenoviral administration, as compared to non-replicative control. No significant difference was observed in tumor volumes between Cox2CRAdΔ E3ADPLuc and WtΔE3ADPLuc treated groups. In Cox2-negative A431 xenografts, only wild-type replication vector (WtΔE3ADPLuc) was capable of suppressing tumor growth, while no statistically significant difference was found between Cox2CRADΔE3ADPLuc and the non-replicative control groups; $*P < 0.05$, $**P < 0.005$, $***P < 0.001$. ADP, adenoviral death protein; CRAd, conditionally replicative adenovirus; Luc, firefly luciferase.

The bioluminescence signals in A431 tumors treated with a Cox2-controlled vector were significantly lower than that with WtΔE3ADPLuc, peaked between day 2 and 5, and disappeared after day 14. Control mice, treated with non-replicative Ad-Cox2LLuc exhibited a barely detectable bioluminescence only within the first week after adenoviral injections (data not shown).

Importantly, analysis of bioluminescence at day 6 following vector administration showed a significant correlation with tumor volumes measured at day 36. Specifically, the mice which showed higher Luc peaks at day 6 after treatment had remarkable tumor shrinkage at day 36 (Fig. 6a,b). Conversely, the mice exhibiting lower levels of bioluminescence at earlier time points demonstrated larger tumor volumes at the end of the experiment. To prove the correlation between produced bioluminescence and therapeutic effect we performed nonparametric Spearman's correlation analysis within each group and then for the combined groups (two vectors combined, two cell lines combined, and overall) (Table 1). The inter-group analysis demonstrated that the bioluminescence levels produced by Cox2CRAdΔE3 ADPLuc and WtΔE3ADPLuc in A549 and A431 tumors were significantly associated with tumor volumes (correlation coefficients, −0.68, −0.93, −0.90, −0.88 respectively). Intra-group analysis performed for both adenoviral vectors within two cell lines also indicated significant negative association between the Luc peaks at day 6 and the tumor volumes at day 36 (correlation coefficient, −0.86; $P < 0.0001$) (Table 1). The correlation between the bioluminescent signal at day 6 and tumor volumes at day 36 was further investigated by a linear regression model for Cox2CRAdΔE3ADPLuc and WtΔE3ADPLuc in A549 and A431 tumor xenografts. The regression analysis also confirmed the significant relationship between early time-point imaging and therapeutic outcome. The estimated regression lines and R^2 are shown in Fig. 6(b).

Discussion

Conditionally replicative adenoviruses (CRAds) kill cancer cells *via* viral replication-dependent cell lysis and exhibit significant *in vivo* and *in vitro* antitumor effects in experimental settings.[1,6,19,23] Nevertheless, the clinical trials performed to date have not shown definitive clinical efficiency as a monotherapy.[5,7,24,25] While recent improvements in developing new generations of oncolytic Ad vectors with enhanced efficacy and specificity are remarkable,[26] noninvasive monitoring of CRAd replication remains a challenge. Currently, invasive, cumbersome biopsy of tumor masses is the standard means used to assess CRAd replication and spread in human clinical trials.[7–9] Clearly, noninvasive imaging of viral replication would provide a simple, easily repeatable, patient-friendly technique for evaluating CRAd distribution and tumor response in patients receiving oncolytic viral therapy. The current work contributes toward this goal.

In order to image dynamically changing viral replication, we designed adenoviral vectors containing MLP-controlled luciferase reporter genes and evaluated how altering vector structure affects the capability of this novel CRAd-based imaging system. Our data lead to two initial conclusions. First, the presence or absence of a polyadenylation signal inserted after the luciferase reporter does not affect viral replication or cytocidal activity in cultured cells, suggesting that the polyadenylation signal does not affect expression of any viral protein located downstream of the Luc cassette. Second, removing the ADP from the adenoviral E3 region impaired viral cytocidal effect, reduced viral replication, and decreased luciferase expression in infected cells. Thus, E3 ADP improves viral spread by provoking efficient viral release from infected cells; this implicates ADP in progeny virion dispersion late in infection.[17,19]

doi: 10.1111/j.1349-7006.2009.01407.x

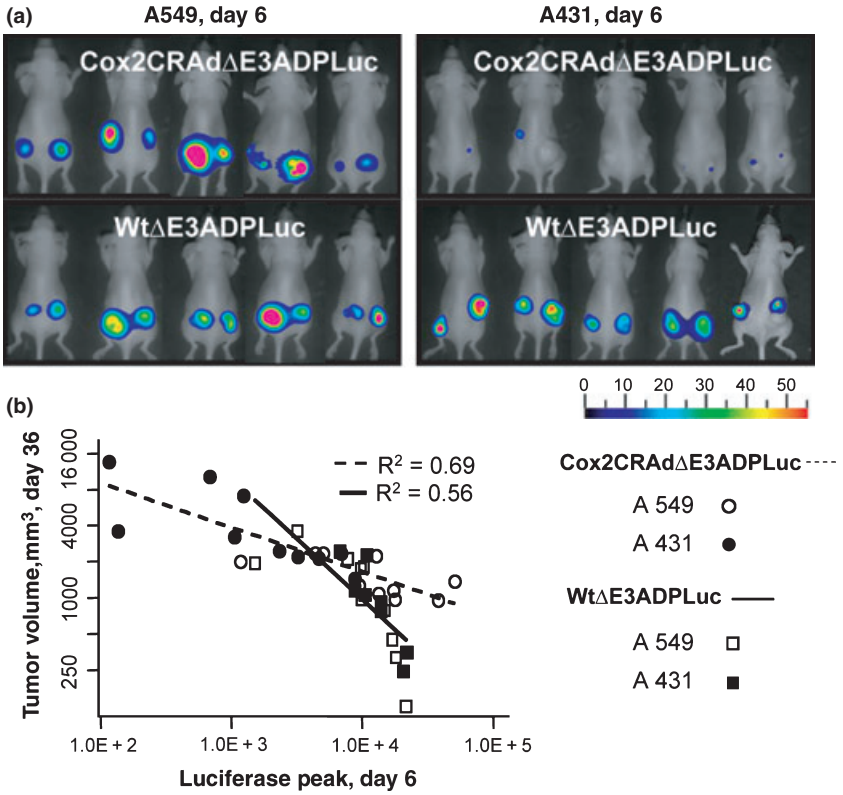

Fig. 6. Bioluminescent imaging of luciferase (Luc) reporter gene can predict the therapeutic outcome of ΔE3Luc oncolytic vectors at earlier time points. (a) Bioluminescent imaging of luciferase reporter in mice bearing A549 or A431 subcutaneous tumors on day 6 after intratumoral treatment with Cox2CRAdΔE3ADPLuc and WtΔE3ADPLuc. (b) Correlation between Luc signal values on day 6 (*x*-axis) and tumor volumes on day 36 (*y*-axis) after adenoviral injections. The *x*- and *y*-axes are shown in natural log scale. The estimated regression lines and R^2 are provided. Regression analysis confirmed significant associations for each group.

Table 1. Spearman correlation between bioluminescence values at day 6 and tumor volumes at day 36 after adenoviral treatment of A549 and A431 tumor xenografts in a nude mouse cancer model

Ad vector	A549 tumors	A431 tumors	A549 and A431 combined
Cox2CRAdΔE3ADPLuc	−0.68*	−0.90***	−0.86***
WtΔE3ADPLuc	−0.93***	−0.88**	−0.89***
Two vectors combined	−0.75***	−0.93***	Overall: −0.86***

*$P < 0.05$, **$P < 0.005$, ***$P < 0.001$. Ad, adenovirus.

Subsequent experiments investigated the expression of luciferase from the adenoviral E3 region in replication-permissive and non-permissive cells. We compared human lung adenocarcinoma A549 cells which support human Ad5 replication with mouse hepatoma BNL-1NG-A.2 cells that do not. Our data show that ΔE3Luc vectors provoked MLP-dependent luciferase expression and subsequent oncolysis only in A549 lung cancer cells but not in mouse hepatoma BNL-1NG-A.2. Importantly, luciferase bioluminescence closely correlated with viral DNA quantity, a direct measure of viral replication, indicating that reporter expression requires viral replication. These data provide strong evidence that adenoviral vectors imbued with Luciferase in the E3 region can report adenoviral replication. It is important to note that the cytolytic effect of Cox2CRAdΔE3ADPLuc was as strong as that of the Ad5 wild-type vector and its reporter signal showed accurate representation of viral replication in the cells with various level of Cox2 promoter activity.

We also determined whether intratumoral or intravenous administration of the Cox2CRAdΔE3ADPLuc CRAd affects its ability to monitor viral replication in A549 subcutaneous xenografts. We found that bioluminescence occurred as early as 1 day after intratumoral administration of CRAds compared to 5 days when the virus was injected systemically. The peak level of bioluminescence also occurred earlier following local administration with signals peaking 5–9 days after intratumoral CRAd administration compared with 13–20 days using the systemic, intravenous route. These data suggest that appropriate ΔE3 vectors can target tumors even with systemic administration, and if those vectors contain suitable imaging capacity, they can effectively report early detection of viral replication and viral distribution within the tumor itself. The ability to accomplish early detection of adenovirus replication in clinics would offer the potential to acquire interval endpoint data with respect to the function of CRAds, a utility not commonly achievable with conventional vector detection techniques. Results obtained with the mouse that developed ascites and metastases may suggest that adenoviral vectors modified to contain sensitive imaging capabilities could also identify small tumor metastases and monitor their response to therapy. However, additional studies (i.e. establishing *in vivo* metastases models) are required to confirm the ability of our system to track and treat metastatic tumor.

Currently, noninvasive imaging modalities offer excellent tools for identifying tumor masses.[27] Imaging has been applied for oncolytic virus replication monitoring.[28,29] The potential of replication-competent adenovirus to enable fluorescent-guided surgical navigation in tumor patients has been recently reported.[30] CRAd vectors with imaging capability, such as those we describe here, may provide insight into virotherapy efficacy by allowing for direct imaging and quantitating of viral replication in early stage cancer. Correlating CRAd replication

with CRAd therapeutic efficacy has not yet been attempted. Such an ability to follow the response to CRAd therapy serially and in real-time may prove extremely useful in the clinical decision-making process. In this regard, a recent study of oncolytic ONYX-015 in colorectal cancer patients demonstrated that an early increase in tumor volume that followed viral treatment occurred because of extensive virus-induced necrosis of tumor masses and not continued tumor growth.[31] Hence, the accurate evaluation of virotherapy efficacy at early disease stages may be crucial to making correct decisions about the subsequent course of therapy. Our data showing that bioluminescent imaging at early time points significantly correlates with CRAd antitumor efficacy indicate that the current approach may aid in improving virotherapy decision-making. In our therapeutic studies, both Cox2CRAdΔE3ADPLuc and WtΔE3ADPLuc provoked high bioluminescence in A549 tumors 6 days after treatment and these mice exhibited a significant tumor shrinkage later, at day 36. Conversely, A431 Cox2-negative tumors treated with Cox2CRAdΔE3ADPLuc demonstrated a weak bioluminescence at day 6 and their therapeutic response was minimal, while WtΔE3ADPLuc resulted in a remarkable final therapeutic outcome after demonstration of high Luc peaks at earlier time points. The detailed statistical analysis relating the luciferase signal intensity at day 6 after treatment to the degree of tumor burden at day 36 showed the significant negative correlation within each treated group, different group combinations, and overall combined samples. This indicates that early time-point imaging, either bioluminescent or by another modality, may predict therapeutic outcome. Of note, the antitumor effect of the Cox2CRAdΔE3ADPLuc and WtΔE3ADPLuc vectors based on tumor volume measurement became significant 18 days after viral administration, suggesting that evaluating vector tumoricidal effect based on changes in tumor size at early time points is not accurate. We believe our data is the first report of the possible predictive value of adenoviral replication imaging.

Further development of the noninvasive imaging technique described here may help both preclinical experiments and clinical CRAd trials. It also will be of interest to determine if noninvasive, serial imaging of *in vivo* CRAd replication can predict tumoricidal efficacy in humans. While luciferase expression and bioluminescence imaging cannot be used in humans, our data provide proof-of-concept that CRAd vectors modified to include high-sensitivity imaging systems like the radionuclide-based somatostatin receptor (SSTR) or human sodium iodide symporter (hNIS) transgenes may improve the outcome of human gene therapy protocols. Bioimaging assessment of viral replication should provide both new information about CRAd biology in humans and an early indication of the tumoricidal effect of oncolytic viral therapy.

Acknowledgments

The authors thank Drs H. Inoue and T. Tanabe for providing a plasmid phPES2 containing the Cox2 promoter. The authors thank Drs Paul Wolkowicz and Mara Oikonomou for extensive help in preparing this manuscript. This project is partly supported by NIH/NIDDK (DK63615 to M.Y.) and NIH/NCI (CA94084 to M.Y. and CA11569 to D.T.C.).

References

1 Alemany R, Balague C, Curiel DT. Replicative adenoviruses for cancer therapy. *Nat Biotechnol* 2000; **18**: 723–7.
2 Verma IM, Weitzman MD. Gene therapy: twenty-first century medicine. *Annu Rev Biochem* 2005; **74**: 711–38.
3 Kirn D. Oncolytic virotherapy for cancer with the adenovirus dl1520 (Onyx-015): results of phase I and II trials. *Expert Opin Biol Ther* 2001; **1**: 525–38.
4 Reid T, Galanis E, Abbruzzese J *et al.* Hepatic arterial infusion of a replication-selective oncolytic adenovirus (dl1520): phase II viral, immunologic, and clinical endpoints. *Cancer Res* 2002; **62**: 6070–9.
5 Alemany R. Cancer selective adenoviruses. *Mol Aspects Med* 2007; **28**: 42–58.
6 Yamamoto M, Curiel DT. Cancer gene therapy. *Technol Cancer Res Treat* 2005; **4**: 315–30.
7 DeWeese TL, van der Poel H, Li S *et al.* A phase I trial of CV706, a replication-competent, PSA selective oncolytic adenovirus, for the treatment of locally recurrent prostate cancer following radiation therapy. *Cancer Res* 2001; **61**: 7464–72.
8 Khuri FR, Nemunaitis J, Ganly I *et al.* A controlled trial of intratumoral ONYX-015, a selectively-replicating adenovirus, in combination with cisplatin and 5-fluorouracil in patients with recurrent head and neck cancer. *Nat Med* 2000; **6**: 879–85.
9 Nemunaitis J, Ganly I, Khuri F *et al.* Selective replication and oncolysis in p53 mutant tumors with ONYX-015, an E1B-55kD gene-deleted adenovirus, in patients with advanced head and neck cancer: a phase II trial. *Cancer Res* 2000; **60**: 6359–66.
10 Ono HA, Le LP, Davydova JG, Gavrikova T, Yamamoto M. Noninvasive visualization of adenovirus replication with a fluorescent reporter in the E3 region. *Cancer Res* 2005; **65**: 10154–8.
11 Zinn KR, Chaudhuri TR, Szafran AA *et al.* Noninvasive bioluminescence imaging in small animals. *Ilar J* 2008; **49**: 103–15.
12 Wu JC, Sundaresan G, Iyer M, Gambhir SS. Noninvasive optical imaging of firefly luciferase reporter gene expression in skeletal muscles of living mice. *Mol Ther* 2001; **4**: 297–306.
13 Ray P, Gambhir SS. Noninvasive imaging of molecular events with bioluminescent reporter genes in living subjects. *Methods Mol Biol* 2007; **411**: 131–44.
14 Ishikawa TO, Jain NK, Taketo MM, Herschman HR. Imaging cyclooxygenase-2 (Cox-2) gene expression in living animals with a luciferase knock-in reporter gene. *Mol Imaging Biol* 2006; **8**: 171–87.
15 Liang Q, Yamamoto M, Curiel DT, Herschman HR. Noninvasive imaging of transcriptionally restricted transgene expression following intratumoral injection of an adenovirus in which the COX-2 promoter drives a reporter gene. *Mol Imaging Biol* 2004; **6**: 395–404.
16 Mittal SK, McDermott MR, Johnson DC, Prevec L, Graham FL. Monitoring foreign gene expression by a human adenovirus-based vector using the firefly luciferase gene as a reporter. *Virus Res* 1993; **28**: 67–90.
17 Doronin K, Toth K, Kuppuswamy M, Krajcsi P, Tollefson AE, Wold WS. Overexpression of the ADP (E3-11.6K) protein increases cell lysis and spread of adenovirus. *Virol* 2003; **305**: 378–87.
18 Mittal SK, Bett AJ, Prevec L, Graham FL. Foreign gene expression by human adenovirus type 5-based vectors studied using firefly luciferase and bacterial beta-galactosidase genes as reporters. *Virol* 1995; **210**: 226–30.
19 Lichtenstein DL, Spencer JF, Doronin K *et al.* An acute toxicology study with INGN 007, an oncolytic adenovirus vector, in mice and permissive Syrian hamsters; comparisons with wild-type Ad5 and a replication-defective adenovirus vector. *Cancer Gene Ther* 2009; **16**:644–54.
20 Yamamoto M, Davydova J, Wang M *et al.* Infectivity enhanced, cyclooxygenase-2 promoter-based conditionally replicative adenovirus for pancreatic cancer. *Gastroenterology* 2003; **125**: 1203–18.
21 Davydova J, Le LP, Gavrikova T, Wang M, Krasnykh V, Yamamoto M. Infectivity-enhanced cyclooxygenase-2-based conditionally replicative adenoviruses for esophageal adenocarcinoma treatment. *Cancer Res* 2004; **64**: 4319–27.
22 Yamamoto M, Alemany R, Adachi Y, Grizzle WE, Curiel DT. Characterization of the cyclooxygenase-2 promoter in an adenoviral vector and its application for the mitigation of toxicity in suicide gene therapy of gastrointestinal cancers. *Mol Ther* 2001; **3**: 385–94.
23 Alemany R. Designing adenoviral vectors for tumor-specific targeting. *Methods Mol Biol* 2009; **542**: 57–74.
24 Kirn D. Clinical research results with dl1520 (Onyx-015), a replication-selective adenovirus for the treatment of cancer: what have we learned? *Gene Ther* 2001; **8**: 89–98.
25 Crompton AM, Kirn DH. From ONYX-015 to armed vaccinia viruses: the education and evolution of oncolytic virus development. *Curr Cancer Drug Targets* 2007; **7**: 133–9.
26 Waehler R, Russell SJ, Curiel DT. Engineering targeted viral vectors for gene therapy. *Nat Rev Genet* 2007; **8**: 573–87.
27 Gambhir SS. Molecualr imaging of cancer: from molecules to humans. Introduction. *J Nucl Med* 2008; **49** (Suppl 2): 1S–4S.
28 Le LP, Everts M, Dmitriev IP, Davydova JG, Yamamoto M, Curiel DT. Fluorescently labeled adenovirus with pIX-EGFP for vector detection. *Mol Imaging* 2004; **3**: 105–16.
29 Carlson SK, Classic KL, Hadac EM *et al.* Quantitative molecular imaging of viral therapy for pancreatic cancer using an engineered measles virus

doi: 10.1111/j.1349-7006.2009.01407.x

expressing the sodium-iodide symporter reporter gene. *AJR Am J Roentgenol* 2009; **192**: 279–87.
30 Kishimoto H, Zhao M, Hayashi K *et al.* In vivo internal tumor illumination by telomerase-dependent adenoviral GFP for precise surgical navigation. *Proc Natl Acad Sci U S A* 2009; **106**: 14514–7.
31 Reid TR, Freeman S, Post L, McCormick F, Sze DY. Effects of Onyx-015 among metastatic colorectal cancer patients that have failed prior treatment with 5-FU/leucovorin. *Cancer Gene Ther* 2005; **12**: 673–81.

Supporting Information

Additional supporting information may be found in the online version of this article:

Fig. S1. Cox2CRAdΔE3ADPLuc showed luminescence-based imaging in spontaneously developed distant metastases in a nude mouse. (a) By day 13 after intratumoral treatment with Cox2CRAdΔE3ADPLuc (4×10^9 vp/tumor), one mouse bearing an A549 subcutaneous xenograft developed ascites, and bioluminescent signal was detected from the abdominal area. (b) On day 20 after adenovirus (Ad) treatment, the mouse was sacrificed after acquiring the whole-body luciferase imaging, and the peritoneal cavity was opened. (c) To confirm the origin of the bioluminescent signal in the peritoneal cavity, the organs were isolated and placed on a petri dish and re-imaged *ex vivo*. The source of bioluminescent signal was from distant tumor metastases in the intestines, stomach, diaphragm, and peritoneum.

Please note: Wiley-Blackwell are not responsible for the content or functionality of any supporting materials supplied by the authors. Any queries (other than missing material) should be directed to the corresponding author for the article.